THE JOURNAL OF PHYSICAL CHEMISTRY B

 VOLUME 107, NUMBER 42, OCTOBER 23, 2003

LETTERS

Cooling-rate Dependent Ferromagnetism in a Two-dimensional Cyano-bridged Sm(III)-W(V) Complex

Toshiya Hozumi,[†] Shin-ichi Ohkoshi,*[,†,‡] Yoichi Arimoto,[†] Hidetake Seino,[§] Yasushi Mizobe,[§] and Kazuhito Hashimoto*[,†]

Research Center for Advanced Science and Technology, The University of Tokyo, 4-6-1 Komaba, Meguro-ku, Tokyo, Japan, PRESTO, JST, 4-1-8 Honcho Kawaguchi, Saitama, Japan, and Institute of Industrial Science, The University of Tokyo, 4-6-1 Komaba, Meguro-ku, Tokyo, Japan

Received: June 6, 2003; In Final Form: August 25, 2003

We report on cooling-rate dependent ferromagnetism in samarium octacyanotungstate, $Sm(H_2O)_5[W(CN)_8]$. X-ray single-crystal structural analysis showed that this compound consists of a two-dimensional cyano-bridged network, in which Sm(III) and W(V) ions are linked in alternating fashion. When the sample was slowly cooled from 300 to 10 K at a cooling rate of -1 K min^{-1}, the magnetization vs temperature curve showed antiferromagnetism with a Néel temperature (T_N) of 3.0 K. Heat capacity measurement and IR spectral variations of the slowly cooled sample suggest that a structural phase transition occurs at 166 K with a change in the coordination geometry of $W(CN)_8$. Conversely, when the sample was placed directly into a sample chamber at $T = 10$ K, ferromagnetism with a Curie temperature (T_C) of 2.8 K was observed. This phenomenon is due to the overcooling effect of the structural phase transition. On the basis of calculations considering interlayer superexchange interactions and interlayer dipole−dipole interactions, the observed cooling-rate dependent ferromagnetism can be understood by a change of the interlayer superexchange interactions.

In the last 10 years, cyano-bridged metal assemblies[1] have been intensively studied from the viewpoint of use as functionalized molecule-based magnets. For example, hexacyanometalate-based magnets are known to exhibit high magnetic phase transition temperatures[2] and various magnetic functionalities.[3,4] Octacyanometalate-based magnets[5] have also drawn attention because they can take on various types of crystal structures and coordination geometries.[6] For typical magnetic materials such as metal alloys and metal oxides, rare-earth metals play an important role, because rare-earth metals can cause a large magnetic anisotropy in magnets due to their orbital angular momentum.[7] In a series of our work, we have designed a novel type of functionalized magnetic material with a cyano-bridged metal assembly incorporating rare-earth metal ions. For example, we have observed a negative coercive field (so-called inverted hysteresis loop) with $Sm_{0.52}Gd_{0.48}[Cr(CN)_6]\cdot 4H_2O$.[4] In this paper, we report on cooling-rate dependent ferromagnetism with a cyano-bridged metal complex composed of $Sm(H_2O)_5[W(CN)_8]$.

A single crystal of $Sm(H_2O)_5[W(CN)_8]$ was prepared by mixing an acetonitrile solution of $Sm(NO_3)_3\cdot 6H_2O$ and an acetonitrile solution of $(Bu_3NH)_3[W(CN)_8]$ (Bu_3N = tributylamine).[8] X-ray single-crystal structural analysis revealed that this system consists of a two-dimensional (2-D) cyano-bridged network, in which Sm(III) and W(V) ions are linked in alternating fashion (Figure 1). The crystal structure is a

* Corresponding authors. E-mail: ohkoshi@fchem.chem.t.u-tokyo.ac.jp, kazuhito@fchem.chem.t.u-tokyo.ac.jp

† Research Center for Advanced Science and Technology, The University of Tokyo.

‡ PRESTO, JST.

§ Institute of Industrial Science, The University of Tokyo.

10.1021/jp0356057 CCC: $25.00
Published on Web 09/27/2003

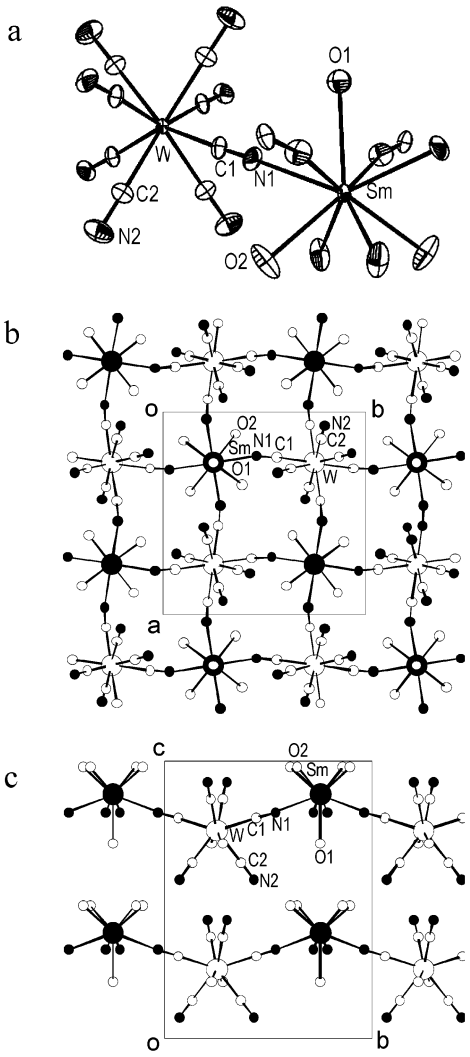

Figure 1. (a) ORTEP drawing of the coordination environments around the W^{V} and Sm^{III} ions for $Sm(H_2O)_5[W(CN)_8]$. Displacement ellipsoids are drawn at a 30% probability level. (b) Projection of the 2-D network in the *ab* plane. (c) Alignment of the 2-D layers along the *c* axis.

tetragonal one of *P*4/*ncc* space group with $a = 10.9203(8)$ Å, $c = 14.658(4)$ Å, and $Z = 4$.[9] Four CN ligands of $W(CN)_8$ are bridged to Sm ions and the other four are free. In contrast, the Sm ion is connected to four cyanonitrogens and five oxygen atoms of water molecules. The coordination geometries around W and Sm ions are close to a square antiprism and a monocapped square antiprism, respectively. The packing mode of the 2-D layers is shown in Figure 1c. W and Sm ions of neighboring layers are related by a *c*/2 translation and the interlayer metal−metal distance (Sm−Sm or W−W) is 7.329 Å. In addition, the distance between the O2 atom of a coordinated water molecule and the N2 atom of free CN group in neighboring layers is 2.854 Å. This short distance suggests the existence of hydrogen bonds between layers.

Magnetic measurements of a powder sample were carried out using a superconducting quantum interference device (SQUID) magnetometer. As the sample was slowly cooled from 300 to 10 K at a cooling rate of -1 K min^{-1}, the magnetization vs temperature curve showed a cusp at 3.0 K (Figure 2a, open circles). The magnetization vs external magnetic field plots below 3 K did not show a hysteresis loop (Figure 2b, open circles). These results indicate that the slowly cooled sample shows antiferromagnetism with a Néel temperature (T_N) of 3.0 K. In contrast, when the sample was placed directly into a

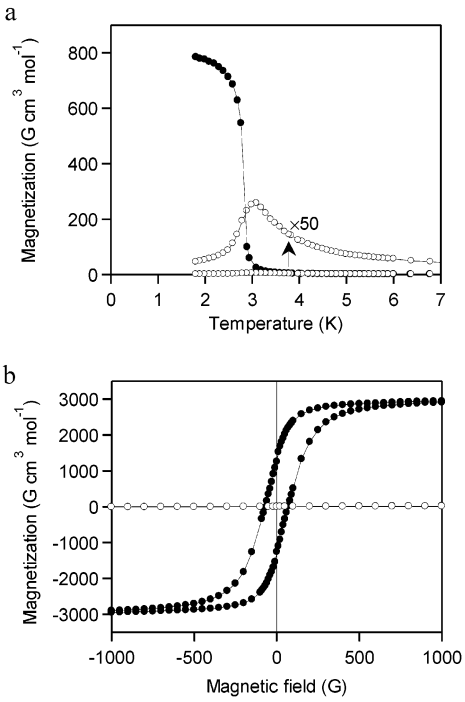

Figure 2. (a) Magnetization vs temperature curves in an external magnetic field of 10 G: (○) the powder sample cooled slowly at a rate of -1 K min^{-1}; (●) the powder sample placed directly into a sample chamber at $T = 10$ K. (b) Magnetic hysteresis loops of the powder sample at 1.9 K: (○) the slowly cooled sample; (●) the rapidly cooled sample.

sample chamber at $T = 10$ K in zero applied magnetic field, a spontaneous magnetization was observed below 2.8 K in the magnetization vs temperature curve in an external field of 10 G (Figure 2a, filled circles). In addition, ac magnetic susceptibility measurements (ac field = 1 G, frequency = 10 Hz) showed a peak in both the real (χ') and the imaginary (χ'') parts at 2.8 K. Furthermore, the magnetization vs external magnetic field plots showed a hysteresis loop with a coercive field of 70 G at 1.9 K (Figure 2b, filled circles). The magnetization value reached 0.95 μ_B at 1.9 K in an external magnetic field of 7 T. The angular dependency of the external magnetic field for a single crystal showed that the magnetic easy-plane of the rapidly cooled sample was almost parallel to the *ab* plane. This magnetic anisotropy is thought to be due to the single-ion anisotropy of the Sm(III) ion. These results indicate that the rapidly cooled sample is a ferromagnet with a Curie temperature (T_C) of 2.8 K.[10] This cooling-rate switching behavior between the ferromagnetic state and antiferromagnetic state was repeatedly observed. For example, the same values of T_C and T_N were observed when the following sequence of SQUID measurements were carried out several times: (first iteration) sample placed directly into a sample chamber of 10 K → (FCM measurement, T_C) → 1.8 K → 300 K → (-2 K min^{-1}) → 10 K → (FCM measurement, T_N) → 1.8 K → remove → (second iteration). Therefore, the observed phenomenon is not due to damage of the sample material under the low-pressure environment inside the SQUID equipment.

To investigate structural variations as a function of temperature, various variable-temperature measurements were carried out. In a heat capacity measurement, the slowly cooled sample revealed an anomalous peak at 166 K (=T_p). The IR spectra were also changed in the vicinity of T_p; i.e., one CN stretching peak due to four bridging CN ligands (A at 2178 cm^{-1}) was split into four peaks (A1, A2, A3, and A4) and the other CN stretching peak due to four free CN ligands (B at 2164 cm^{-1})

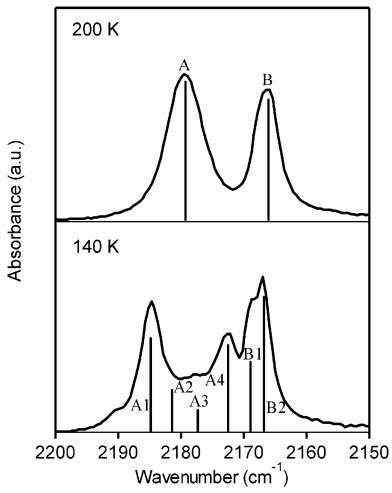

Figure 3. IR spectra of the slowly cooled sample at 200 and 140 K. Two CN stretching peaks due to four bridging CN ligands (**A**) and four free CN ligands (B) were split into four peaks (A1, A2, A3, and A4) and two peaks (B1 and B2), respectively.

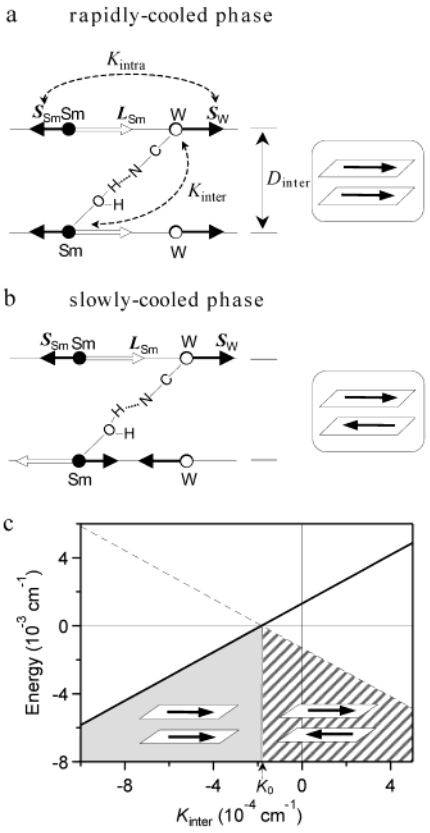

Figure 4. Schematic illustrations of magnetic orderings with L_{Sm}, S_{Sm}, and S_W: (a) ferromagnetic ordering between layers and (b) antiferromagnetic ordering between layers. K_{intra} is the intralayer superexchange coupling constant through bridging cyano groups, and K_{inter} is the interlayer superexchange coupling constant through hydrogen bonds. D_{inter} is the interlayer magnetic dipole−dipole interaction. (c) Magnetic energy of the interlayer magnetic interaction as a function of K_{inter} based on eq 1. Note that zero on the vertical axis means the energy for no interaction between layers. The solid line and the dotted line represent the energies of ferromagnetic ordering (gray area) and antiferromagnetic ordering (lined area), respectively.

was split into two peaks (B1 and B2) around T_p (Figure 3). Simultaneously, a sharp OH stretching peak was also observed around 3400 cm^{-1}. These IR spectral variations indicate that the structural phase transition at T_p is caused by a change in the coordination geometry of $W(CN)_8$. Because X-ray single crystal structural data suggest the existence of hydrogen bonds between layers, the structural phase transition is considered to be caused by the stabilization of hydrogen bonds between 2-D layers. In contrast, when the sample was placed directly into a liquid N2 dewar, its IR spectra at 77 K were similar to the spectra at room temperature. This indicated that, in the rapidly cooled sample, the structure at room temperature was maintained even at low temperature; i.e., the rapidly cooled sample took on an overcooled phase.

We considered the possible mechanism of this cooling-rate dependent ferromagnetism. The angular dependency of the external magnetic field for a single crystal showed that the magnetic anisotropy is not uniaxial and the easy-plane is almost parallel to the *ab* plane. This suggests that magnetic ordering of this system is not due to the 2-D Ising system. Hence, bulk magnetization is caused by three-dimensional (3-D) magnetic ordering, including an interlayer magnetic interaction. That is, in the present system, the switching between ferromagnetic and antiferromagnetic ordering is determined by the change of the magnetic interaction between layers. To clearly understand magnetic interaction between layers, not only the superexchange interaction but also dipole−dipole interaction are considered. The ferromagnetic behavior in the rapidly cooled sample suggests that the intralayer superexchange interaction (K_{intra}) between Sm(III) and W(V) ($S_W = {}^1/_2$) is negative ($K_{intra} < 0$) because, in the Sm(III) ion, orbital angular moment (L_{Sm}) and spin angular moment (S_{Sm}) are antiparallel ($L_{Sm} = 5$, $S_{Sm} = 5/2$, $J_{Sm} = L_{Sm} - S_{Sm} = {}^5/_2$) (Figure 4a). In addition, the magnetization direction was parallel to the *ab* plane. In such a case, the magnetic ordering is determined by the interlayer dipole−dipole interaction (D_{inter})[11] and the interlayer superexchange interaction (K_{inter}), and hence, we calculated the sum of energies of D_{inter} and K_{inter} using the point−dipole approximation and molecular field theory, respectively. The atomic positions of the Sm and W were set, on the basis of the observed atomic positions of crystal structure. The total energy (E) of the interlayer magnetic interactions at 0 K is expressed by the combination of D_{inter} and K_{inter} as follows:

$$E = \frac{1}{4\pi\mu_0}\sum_{i,j}\frac{1}{r^3}\left[(\mathbf{M}_i\cdot\mathbf{M}_j) - \frac{3(\mathbf{M}_i\cdot\mathbf{r})(\mathbf{M}_j\cdot\mathbf{r})}{r^2}\right] - \frac{2Z(g_{Sm}-1)}{g_{Sm}g_W{\mu_B}^2}K_{inter}\mathbf{M}_{Sm}\cdot\mathbf{M}_W \quad (1)$$

where i is Sm^{III} or W^V and j is nearest Sm^{III} or W^V in the neighboring layer, r is the distance between i and j sites, μ_0 is the permeability of a vacuum, μ_B is the Bohr magneton, Z is the number of Sm ions connected to a W ion through hydrogen bonds ($Z = 4$), and g_{Sm} and g_W are Landé g factors of Sm and W ions, respectively. Numerical calculations were carried out under the condition that the magnetic ordering between layers is parallel or antiparallel. Figure 4c shows the magnetic energies of parallel ordering (solid line) and antiparallel ordering (dotted line) as a function of K_{inter}. Note that zero on vertical axis means the energy for no interaction between layers. In the range of $K_{inter} < -1.8 \times 10^{-4}$ cm^{-1} ($=K_0$), parallel magnetic ordering between layers is stable. On the other hand, in the range of $K_{inter} > K_0$, antiparallel magnetic ordering between layers is suitable. Hence, the switching behavior between the rapidly cooled and slowly cooled samples will be caused by the change of K_{inter}, which are due to the variation of coordination geometry of $W(CN)_8$. It is considered that the difference in interlayer

superexchange pathways through hydrogen bond contributes to the change of K_{inter}.

In summary, we have prepared a novel type of 2-D cyano-bridged complex composed of $Sm(H_2O)_5[W(CN)_8]$. In this system, as the sample was slowly cooled, antiferromagnetism was observed, whereas as the sample was rapidly cooled, ferromagnetism was observed. This phenomenon is caused by a combination of the magnetic anisotropy of Sm ions and the geometrical flexibility of octacyanometalates. A similar phenomenon was observed in only one material of $[(C_2H_5)_4N][FeCl_4]$ twenty years ago, although its mechanism is different from that of our system.[12]

Acknowledgment. The present research is supported in part by a Grant for 21st Century COE Program "Human-Friendly Materials based on Chemistry" from the Ministry of Education, Culture, Sports, Science, and Technology of Japan.

Supporting Information Available: An X-ray crystallographic file (CIF). This material is available free of charge via the Internet at http://pubs.acs.org.

References and Notes

(1) (a) Verdaguer, M.; Bleuzen, A.; Marvaud, V.; Vaissermann, J.; Seuleiman, M.; Desplanches, C.; Scuiller, A.; Train, C.; Garde, R.; Gelly, G.; Lomenech, C.; Rosenman, I.; Veillet. P.; Cartier, C.; Villain, F. *Coord. Chem. Rev.* **1999**, *192*, 1023. (b) Hashimoto, K.; Ohkoshi, S. *Philos. Trans. R. Soc. London, Ser. A* **1999**, *357*, 2977. (c) Miller, J. S. *MRS Bull.* **2000**, *25*, 60. (d) Ohba, M.; Okawa, H. *Coord. Chem. Rev.* **2000**, *198*, 313. (e) Smith, J. A.; Galan-Mascaros, J. R.; Clerac, R.; Sun, J. S.; Xiang, O. Y.; Dunbar, K. R. *Polyhedron* **2002**, *20*, 1727.

(2) (a) Ferlay, S.; Mallah, T.; Ouahs, R.; Veillet, P.; Verdaguer, M. *Nature* **1995**, *378*, 701. (b) Holmes, S. M.; Girolami, G. S. *J. Am. Chem. Soc.* **1999**, *121*, 5593. (c) Hatlevik, Ø.; Bushmann, W. E.; Zhang, J.; Manson, J. L.; Miller, J. S. *Adv. Mater.* **1999**, *11*, 914.

(3) (a) Sato, O.; Iyoda, T.; Fujishima, A.; Hashimoto, K. *Science* **1996**, *272*, 704. (b) Ohkoshi, S.; Iyoda, T.; Fujishima, A.; Hashimoto, K. *Phys. Rev. B* **1997**, *56*, 11642. (c) Ohkoshi, S.; Abe, Y.; Fujishima, A.; Hashimoto, K. *Phys. Rev. Lett.* **1999**, *82*, 1285. (d) Pejakovic, D. A.; Manson, J. L.; Miller, J. S.; Epstein, A. J. *J. Appl. Phys.* **2000**, *87*, 6028.

(4) Ohkoshi, S.; Hozumi, T.; Hashimoto, K. *Phys. Rev. B* **2001**, *64*, 132404.

(5) (a) Garde, R.; Desplanches, C.; Bleuzen, A.; Veillet, P.; Verdaguer, M. *Mol. Cryst. Mol. Liq. Cryst.* **1999**, *334*, 587. (b) Ohkoshi, S.; Machida, N.; Zhong, Z. J.; Hashimoto, K. *Synth. Met.* **2001**, *122*, 523. (c) Rombaut, G.; Verelst, M.; Golhen, S.; Ouahab, L.; Mathoniere, C.; Kahn, O. *Inorg. Chem.* **2001**, *40*, 1151. (d) Zhong, Z. J.; Seino, H.; Mizobe, Y.; Hidai, M.; Fujishima, A.; Ohkoshi, S.; Hashimoto, K. *J. Am. Chem. Soc.* **2000**, *122*, 2952. (e) Larionova, J.; Gross, M.; Pilkington, M.; Andres, H.; Stoeckli-Evans, H.; Güdel, H. U.; Decurtins, S. *Angew. Chem., Int. Ed. Engl.* **2000**, *39*, 1605. (f) Zhong, Z. J.; Seino, H.; Verdaguer, M.; Ohkoshi, S.; Hashimoto, K. *Inorg. Chem.* **2000**, *39*, 5095. (g) Arimoto, Y.; Ohkoshi, S.; Zhong, Z. J.; Seino, H.; Mizobe, Y.; Hashimoto, K. *Chem. Lett.* **2002**, 832. (h) Yokoyama, T.; Okamoto, K.; Ohta, T.; Ohkoshi, S.; Hashimoto, K. *Phys. Rev. B* **2002**, *65*, 064438. (i) Podgajny, R.; Korzeniak, T.; Balanda, M.; Wasiutynski, T.; Errington, W.; Kemp, T. J.; Alcock, N. W.; Sieklucka, B. *Chem. Commun.* **2002**, 1138. (j) Li, D.; Gao, S.; Zheng, Li.; Tang, W. *J. Chem. Soc., Dalton Trans.* **2002**, 2805.

(6) Leipoldt, J. G.; Basson, S. S.; Roodt, A. *Adv. Inorg. Chem.* **1993**, *40*, 241.

(7) Chikazumi, S. *Physics of Magnetism*; Weily & Sons: New York, 1964.

(8) Elemental analyses by inductively coupled plasma mass spectrometry and standard microanalytical methods showed that the formula of the precipitate obtained was $Sm(H_2O)_5[W(CN)_8]$. Calcd: Sm, 23.78; W, 29.06; C, 15.19; H, 1.59; N, 17.72. Found: Sm, 24.17; W, 29.25; C, 15.01; H, 1.69; N, 17.71%.

(9) All measurements were performed on a Rigaku AFC7R diffractometer with a Mo Kα source at room temperature. The structures were solved by Patterson methods, expanded by Fourier synthesis, and refined by full-matrix least-squares techniques by using SHELXL-97. Crystallographic data for $Sm(H_2O)_5[W(CN)_8]$: $C_8N_8H_{10}O_5SmW$, fw = 632.47, tetragonal, *P*4/*ncc* (No. 130), $a = 10.9203(8)$ Å, $c = 14.658(4)$ Å; $V = 1748.0(4)$ Å^3; $Z = 4$; $D_{calcd} = 2.403$ g/cm^3, μ(Mo Kα) = 99.5 cm^{-1}, $R = 0.037$ and $R_W = 0.132$ for 629 unique reflections ($I > 3\sigma(I)$) and 56 parameters.

(10) As for Sm(III) ion, orbital angular moment (L_{Sm}), spin angular moment (S_{Sm}), total angular moment ($J_{Sm} = L_{Sm} - S_{Sm}$), and Landé *g* factor (g_{Sm}) are 5, $^5/_2$, $^5/_2$, and $^2/_7$, respectively, and hence, the sublattice magnetization of Sm site is 0.71 μ_B ($=g_{Sm}J_{Sm}$). As for the W(V) ion, because the spin angular moment (S_W) is $^1/_2$, the sublattice magnetization of W is 1.0 μ_B. At 0 K, when the sublattice magnetizations of Sm and W are antiparallely ordered, the expected M_s value is 0.29 μ_B. In contrast, in the case of the parallel ordering, the expected M_s value is 1.71 μ_B. Hence, the observed M_s value of 0.95 μ_B suggests that this compound is not a ferromagnet. However, the observed magnetization value of 0.95 μ_B is smaller than the expected ferromagnetic M_s value of 1.71 μ_B. One of the reasons is that the measuring temperature is not low enough compared to the T_C value of 2.8 K. The theoretical M_s value at 1.9 K can be estimated to be 1.37 μ_B from the calculation based on the molecule field theory. Another reason is that the measured sample is powder form, and hence, the magnetization value cannot saturate by the applied magnetic field of 7 T due to a large magnetic anisotropy of the Sm ion.

(11) (a) Wynn, C. M.; Gîrtu, M. A.; Brinckerhoff, W. B.; Sugiura, K.; Miller, J. S.; Epsterin, A. J. *Chem. Mater.* **1997**, *9*, 2156. (b) Drillon, M.; Panissod, P. *J. Magn. Magn. Mater.* **1998**, *188*, 93.

(12) (a) Puertolas, J. A.; Navarro, R.; Palacio, F.; Gonzalez, D.; Carlin R. L.; van Duyneveldt, A. J. *J. Magn. Magn. Mater.* **1983**, 31−34, 1067. (b) Puertolas, J. A.; Orera, V. M.; Palacio, F.; van Duyneveldt, A. J. *Phys. Lett.* **1983**, *98A*, 374.